Research Journal of Chemical Sciences _____ ISSN 2231-606X
Vol. **3(10),** 56-63, October **(2013)** *Res. J. Chem. Sci.*

Kinetic Investigations of the Hydrogen evolution reaction on Hg electrode: Impedance Spectroscopy studies

Jafarian M.[1], Behazin M.[2], Danaee I.[3] and Gobal F.[4]
[1]Department of Chemistry, K. N. Toosi University of Technology, Tehran, IRAN
[2]Department of Chemistry, The University of Western Ontario, London, Ontario, CANADA
[3]Abadan Faculty of Petroleum Engineering, Petroleum University of Technology, Abadan, IRAN
[4]Department of Chemistry, Sharif University of Technology, Tehran, IRAN

Available online at: www.isca.in, www.isca.me
Received 1st September 2013, revised 16th September 2013, accepted 17th October 2013

Abstract

The mechanism and kinetics of the hydrogen evolution reaction (HER) on Hg electrode in 0.1 M H_2SO_4 solution were studied using steady-state polarization, open circuit potential transient and electrochemical impedance. The simulation of the data obtained from these methods, by nonlinear fitting procedure allowed us to determine the rate constants of the Volmer, Heyrovsky and Tafel steps associated with the hydrogen evolution reaction. The kinetics results indicate that HER mechanism at low negative potentials is a serial combination of Volmer and parallel Tafel and Heyrovsky steps. At high negative potentials where the hydrogen coverage reaches its limiting value, a Tafel line with the slope of -116 mV dec^{-1} is obtained. In this potential hydrogen evolution follows the Volmer-Heyrovsky mechanism while the Tafel step has negligible contribution. Open circuit potential for Hg at different charging currents show that the higher charging cathodic current, the longer time is required to reach the equilibrium potential.

Keywords: Impedance; hydrogen evolution; mercury; equivalent circuit.

Introduction

Hydrogen evolution reaction (HER) is one of the most intensively studied reactions in electrochemistry. The study of hydrogen evolution is of primary importance in the area of metal hydride batteries[1,2], hydrogen production through water electrolysis[3], fuel cells based on hydrogen fuel[4,5] and even in the inhibition of hydrogen embrittlement[6]. The reduction reaction mechanisms of different species have been investigated on mercury electrode and the kinetic and thermodynamic parameters have been evaluated[7-11]. Hydrogen evolution reaction was contributed in reduction as parallel reaction on Hg electrode. Ohsaka et al.[12] studied the kinetic behavior of oxygen reduction on mercury electrode. The parallel electroreduction of some metal cations and H^+ ions at the mercury electrode was investigated by Orlik et al.[13].

The relation between the kinetics parameters, the coverage of adsorbed hydrogen and the overpotential has also been the subject of a good number of theoretical works[14]. The measurement of potential relaxation at open-circuit following the interruption of a polarizing current provides[15,16] data leading to information on the interfacial capacitance of the electrode. The determination of the dependency of the surface coverage by the reaction intermediate is another important feature of the kinetics of the hydrogen evolution needed for the better understanding of the reaction mechanism[17].

In cases where steady-state coverage by adsorbed intermediates is appreciable, this leads to potential dependence of the coverage by these intermediates, i.e., an adsorption pseudocapacitance is generated[18,19]. Probably the most striking effect observed experimentally at a mercury electrode is the appearance of Tafel behavior in a wide region of the electrode overpotentials[20].

Electrochemical impedance spectroscopy (EIS) is a good tool for the analysis of the kinetics of electrode reactions. The advantage of EIS over DC techniques is that this steady-state technique is capable of probing relaxation phenomena over a wide frequency range. The measured impedance can be presented in the form of imaginary vs. real parts at various measurement frequencies, Nyquist plots, which appear as a multitude of semi-circles and lines[21]. Equivalent electrical circuits responding to potential stimuli to generate the same impedance plots are used for the interpretations of the results and associate kinetics and transport properties with the circuit elements. Often, discrepancies and ambiguities hamper the analysis[21] as several apparently different equivalent circuits may show the same impedance characteristics and supplementary data and chemical intuition then help to select the most relevant one. Also, it may be difficult to find electrochemical equivalent to some electrical circuit elements and vice versa[21,22].

Numerous investigations have been done on HER and its fundamental issues on various metals[23-25]. This work is devoted

to the investigation of kinetic of HER on mercury electrode. The simulation of the experimental impedance along with analyzing the steady-state polarization data and open circuit potential transient diagrams in terms of the Volmer–Heyrovsky–Tafel steps allow us to estimate the kinetic parameters of the HER on mercury.

Materials and Methods

The electrochemical experiments were performed in the 0.1 M H_2SO_4 solution. Sulfuric acid used in this work was Merck product (No. 112080) of analytical grade and was used without further purification. The electrolyte was purged by nitrogen to remove dissolved air. All studies were carried out at 298 ± 2K. Electrochemical studies were carried out in a conventional three electrode cell where a saturated Ag/AgCl electrode and a Pt wire were used as the reference and counter electrodes, respectively. All potentials are referred to the standard hydrogen electrode scale (SHE).

The cell was powered by an electrochemical system comprising of potentiostat/galvanostat EGandG model 273A and frequency response detector EGandG model 1025. The system was run by a PC through M270 and M398 commercial software's via a GPIB interface. The frequency range of 100 kHz to 10 mHz and the modulation of AC amplitude of 10 mV were employed for impedance studies. Open circuit potential measurements were performed for 500 s by a potentiostat/galvanostat Solarton model 1266. The system is run by a PC through corrware commercial software's via a GPIB interface. Open circuit potential decay was measured after the interruption of 500 s applied cathodic polarization current. Steady-state data were obtained potentiostatically in the potential range of -1.078 to -1.248 V point by point, with good reproducibility of measurements. Derived impedance equation was fitted on experimental impedance diagrams and all kinetic parameters were obtained. Fitting of impedance equation and also the proposed equivalent circuit to the experimental impedance spectroscopy data were done by means of home written least square software based on the Marquardt method for the optimization of functions and Macdonald weighting for the real and imaginary parts of the impedance[26,27].

Results and Discussion

A typical steady-state polarization curve for the HER, obtained by the polarization measurement in the potential range of -1.078 to -1.248 V on Hg electrode in 0.1 M H_2SO_4, is presented in figure 1a. A straight line with the slope of -116 mV dec^{-1} has been obtained. The Tafel slope at high negative potentials is close to the theoretical value of -118 mV dec^{-1}, which indicates that, HER proceeds via a Volmer-Heyrovsky mechanism[28].

The mechanism of the HER in aqueous acid solutions is treated as a combination of three basic steps, two electrochemical and one chemical:

$$M + H_3O^+ + e^- \leftrightarrows MH_{ads} + H_2O \quad (1)$$

$$MH_{ads} + H_3O^+ \leftrightarrows M + H_2 + H_2O \quad (2)$$

$$MH_{ads} + MH_{ads} \leftrightarrows H_2 + 2M \quad (3)$$

On this basis the kinetics of HER can be expressed as

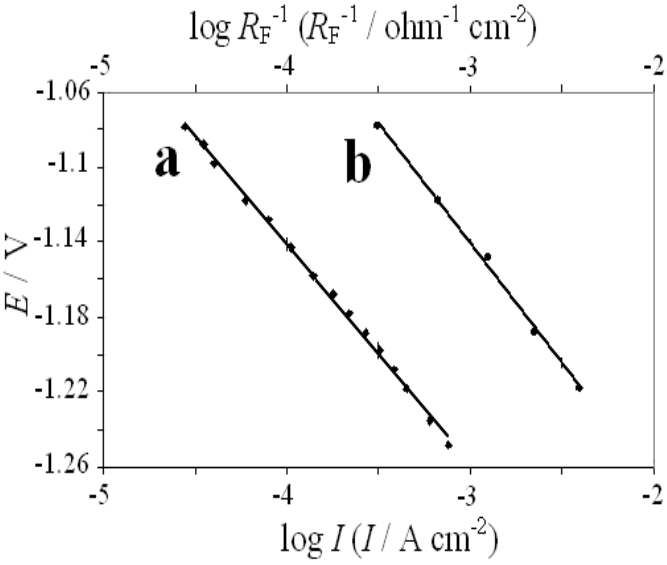

Figure-1 (a)

Steady-state polarization curve of Hg electrode in 0.1 M H_2SO_4; (b) variation of electrode's potential with respect to log $(R_F)^{-1}$ for the HER on Hg electrode in 0.1 M H_2SO_4 solution, according to impedance measurements and data taken from Table-1

$$v_1 = k_1^o C_H (1-\theta)\exp\left(-\frac{E}{b_1}\right) - k_{-1}^o \theta \exp\left(\frac{E}{b_{-1}}\right) \quad (4)$$

$$v_2 = k_2^o C_H \theta \exp\left(-\frac{E}{b_2}\right) - k_{-2}^o (1-\theta)\exp\left(\frac{E}{b_{-2}}\right) \quad (5)$$

$$v_3 = k_3\theta^2 - k_{-3}(1-\theta)^2 \quad (6)$$

In these rate laws θ surface concentrations of the intermediate H_{ads} and the corresponding free adsorption sites at the electrode are given as 1-θ, k_i (mol cm^{-2} s^{-1}) are rate constants, b_i (i=1, -1, 2, -2, 3, -3) the Tafel slope, C_H the H_3O^+ concentration and v_i is the reaction rate.

The steady-state kinetics of the HER at constant current density is characterized by the conditions of the charge balance (with rates in mol cm^{-2} s^{-1}):

$$r_o = \frac{i}{F} = -(v_1 + v_2) \quad (7)$$

and the mass balance with respect to the intermediate H_{ads}:

$$r_1 = \frac{q}{F}\frac{d\theta}{dt} = v_1 - v_2 - 2v_3 \quad (8)$$

q is the charge corresponding to a monolayer coverage by adsorbed hydrogen.

When a particular value of the mass balance, r_1=0 is set, the steady-state coverage can be calculated, assuming that the Langmuir adsorption isotherm is operable. Calculations indicated that the rate constants k_{-2} and k_{-3} of the reverse reactions of steps 2 and 3 could be neglected because they have no significant effect on the reaction rates of the second (Eq. 5) and third step (Equation. 6) at applied over potential range, and the steady state coverage (θ), of the intermediate H_{ads} species is the following function of the corresponding rate constants:

$$\theta = \frac{-(k_1 C_H + k_{-1} + k_2 C_H) + \sqrt{(k_1 C_H + k_{-1} + k_2 C_H)^2 + 8k_1 k_3 C_H}}{4k_3} \quad (9)$$

The presence of the electrochemical rate constants in equation (9) clearly indicates the complex dependence of θ on the electrode potential.

The electrochemical impedance measurements were carried out on Hg electrode in the mentioned potential domain in which the steady-state conditions were ensured and kinetic parameters could be calculated from the Tafel equation.

Figure 2a shows the Nyquist diagrams of Hg electrode recorded at various cathodic overpotential in 0.1 M of H_2SO_4 solution. It is observed that Nyquist diagrams consist of two overlapped capacitive loops which are slightly depressed towards the real axis. The high frequency loop can be related to the combination of charge transfer resistance and the double layer capacitance. The semicircle in the low frequency region was related to the adsorption of reaction intermediate on the electrode surface[29]. Bode Phase diagrams for the same system is shown in figure 2b. Two distinguishable peaks are observed in the Bode plots corresponding to the two depressed semicircle appearing in Nyquist plots. The equivalent circuit compatible with the Nyquist diagram is depicted in figure 3. To obtain a satisfactory impedance simulation of hydrogen evolution it is necessary to replace the capacitor, *C*, with a constant phase element (*CPE*) *Q* in the equivalent circuit. The most widely accepted explanation for the emergence of *CPE* behavior, depressed semicircles, is microscopic roughness on solid electrodes causing an inhomogeneous distribution in the solution resistance as well as in the double-layer capacitance[30-32]. However, for liquid electrode the fitting procedure indicated that when *CPE* was employed, figure 2, a better agreement between equivalent circuit and experimental data was obtained. The impedance of the *CPE* is defined as $Z_{CPE} = 1/T(jw)^n$, where *T* is a capacity parameter and *n* is a dimensionless parameter related to the constant phase angle.

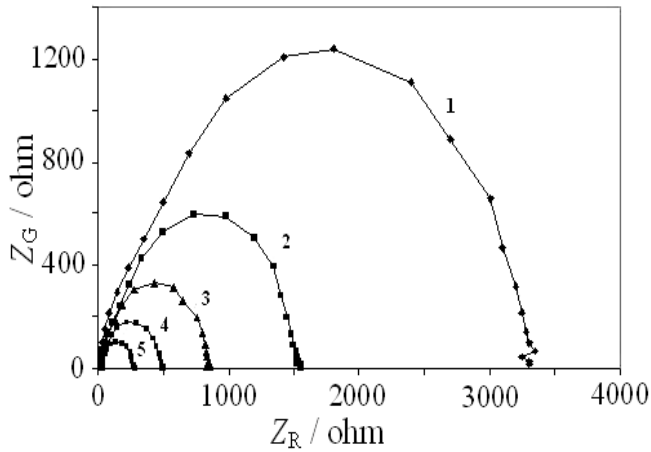

Figure-2a

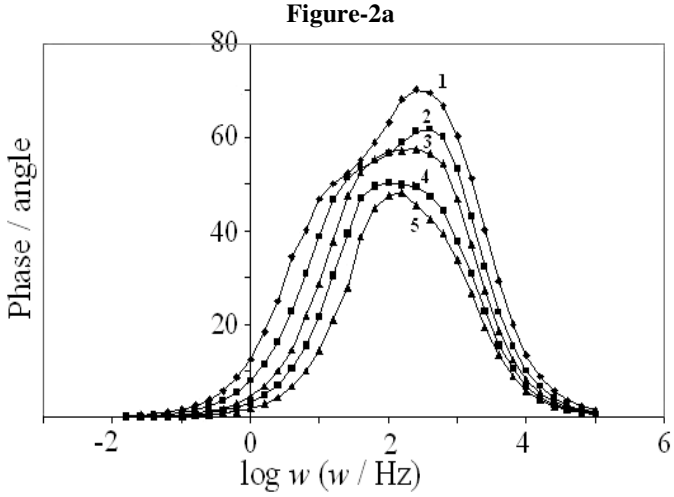

Figure-2b

Figure-2 (a) Presentation of the Nyquist diagrams (b) phase shift plot of Hg electrode in 0.1 M H_2SO_4 at various electrodes' potentials, (1) -1.078, (2) -1.118, (3) -1.148, (4) -1.188 and (5) -1.218 V

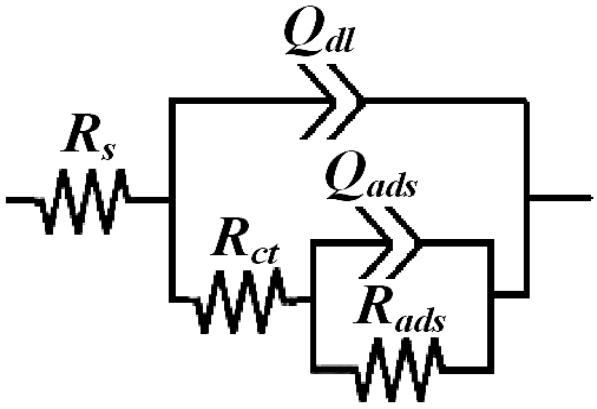

Figure-3

Equivalent circuits compatible with the experimental impedance data in Fig. 2 for hydrogen evolution reaction on Hg electrode

Table-1
Equivalent circuit parameters of hydrogen evolution reaction on Hg electrode in 0.1 M H_2SO_4 solution obtained from figure 2

E / V	R_s / Ω	R_1 / Ω	$Q_1\times10^5$ / F	R_2 / Ω	$Q_2\times10^5$ / F	n_1	n_2
-1.078	19.5	760	2.9	2440	7.9	0.82	0.89
-1.118	20	310	3.9	1190	9	0.89	0.93
-1.148	20	176	5	630	9.2	0.81	0.93
-1.188	19.2	84	6.1	360	11.9	0.92	0.91
-1.218	20	52	7	200	13	0.9	0.91

In this equivalent electrical circuit, R_s, CPE_{dl} and R_{ct} represent solution resistance, a constant phase element corresponding to the double layer capacitance and the charge transfer resistance. CPE_{ads} and R_{ads} are the electrical elements related to the adsorption of reaction intermediates. R_{ads} is actually the inverse of the rate constant of the intermediates adsorption and therefore decreases with increasing the applied cathodic potential. In this circuit the charge transfer resistance of the electrode reaction is the circuit element that has a simple physical meaning describing how fast the rate of charge transfer during hydrogen evolution reaction changes with changing electrode potential when the surface coverage of the intermediate is held constant.

To corroborate equivalent circuit the experimental data are fitted to equivalent circuit and the circuit elements are obtained. Table 1 illustrates the equivalent circuit parameters for the impedance spectra of HER in different applied cathodic potential. It can be seen from figure 2a, with increasing applied cathodic potential decrease the diameters of semicircles.

The sum of the values of the charge transfer and adsorption resistances in impedance measurements at each overpotential demonstrates the total Faradaic resistance (R_F) of the electrode process[33]. The Faradaic resistance at any overpotential is related to the Faradaic current density. So, a plot of electrode potential versus log $(R_F)^{-1}$ should be linear and the corresponding slope is equal to the Tafel slope. Figure 1b shows that data obtained by impedance spectroscopy give a linear relationship for electrode potential versus log $(R_F)^{-1}$ with the slope of b=-0.11 V dec^{-1}. This value is close to the Tafel slope obtained by polarization measurement.

Figure 1 shows both the *E vs.* log *i* and *E vs.* log $(R_F)^{-1}$ plots as two parallel lines separated at the abscissa by the value of 1.39. At sufficiently high negative overpotentials when adsorbed hydrogen coverage is almost constant and for the Langmuir adsorption isotherms of hydrogen, the theoretical separation between the above parallel lines at T=298 K and α=0.5 is expected[33] to be equal to log $(\alpha F/RT)$=1.29 which is close to the experimentally observed separation between the two lines. So, based on theoretical analysis[33] and experimental values, Langmuirian adsorption of hydrogen is presumed on Hg electrode.

Based on the hydrogen evolution mechanism, the Faradaic current density (I_F) can be written as:

$$I_F = (v_1 + v_2)F \tag{10}$$

In the steady state conditions, the Faradaic current density (I_F) of HER can be expressed as a function of the surface coverage of reaction intermediates (θ) and the electrode potential. If a sufficiently small perturbation signal, $\Delta E=|\Delta E|exp(jwt)$, was applied to the electrode, the deviation of I_F from the steady state condition can be approximated by the first order of the Tailor's series expansion:

$$\Delta I_F = \left(\frac{\partial I_F}{\partial E}\right)\Delta E + \left(\frac{\partial I_F}{\partial \theta}\right)\Delta\theta \tag{11}$$

The ratio $\Delta I_F/\Delta E$ is defined as the Faradaic admittance Y_F (inverse of the Faradaic impedance), thus

$$Y_F = \left(\frac{1}{R_t}\right) + \left(\frac{\partial I_F}{\partial \theta}\right)\left(\frac{\Delta\theta}{\Delta E}\right) \tag{12}$$

R_t is the charge transfer resistance of the electrode reaction and its value is always positive. On the basis of reaction mechanism and taking the linear approximation of Tailor's series expansion around the steady state, one has theoretical impedance were obtained (eq.13) and the kinetic constant are determined by fitting the model to the experimental Nyquist diagram (table 2).

$$Y = \left(\frac{1}{\left(\frac{k_1C_H(1-\theta)}{b_1} - \frac{k_{-1}\theta}{b_{-1}} + \frac{k_2C_H\theta}{b_2} - \frac{k_{-2}(1-\theta)}{b_{-2}}\right)F}\right) + \left(-k_1C_H - k_{-1} + k_2C_H + k_{-2}\right) + \frac{F^3\left(\frac{k_1C_H(1-\theta)}{b_1} - \frac{k_{-1}\theta}{b_{-1}} - \frac{k_2C_H\theta}{b_2} + \frac{k_{-2}(1-\theta)}{b_{-2}}\right)}{\left(q\left(-\frac{(-k_1C_H - k_{-1} - k_2C_H - k_{-2} - 4k_3\theta - 4k_{-3}(1-\theta))F}{q} + jw\right)\right)} \tag{13}$$

where q are charges required for complete adsorption of the intermediate on unit surface.

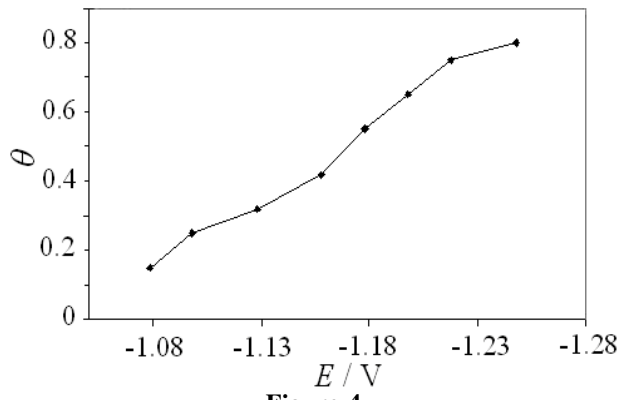

Figure-4
Potential dependence of the calculated values of the surface coverage (θ) by adsorbed hydrogen

Table-2
Values of rate constant calculated from Eq. 13 and figure 2 for hydrogen evolution reaction on Hg electrode in 0.1 M H_2SO_4 solution.

$k_1^o \times 10^{21}$ / mol cm^{-2} s^{-1}	$k_{-1}^o \times 10^4$ / mol cm^{-2} s^{-1}	$k_2^o \times 10^{21}$ / mol cm^{-2}s^{-1}	$k_{-2}^o \times 10^5$ / mol cm^{-2} s^{-1}	$k_3 \times 10^{10}$ / mol cm^{-2} s^{-1}	$k_{-3} \times 10^{11}$ / mol cm^{-2} s^{-1}
3.1	*2*	*1*	*4.5*	*8.1*	*8*

The coverage of reaction intermediate, as a function of over potential can be obtained from the model calculation and is presented in figure 4. With the increase of over potential, the values of the calculated surface coverage increased and approach the limiting value of 0.8.

Comparing the theoretical Faradaic impedance, equation. (13), and the equivalent circuit, the relations between the elements R_{ct}, R_{ads} and Q_{ads} and their corresponding electrochemical equivalent were established. These relations were shown in the following system of equations:

$$R_{ct} = R_t \tag{14}$$

$$R_{ads} = \frac{m_2 m_3 R_t^2}{-m_2 m_3 R_{ct} + m_1} \tag{15}$$

$$C_{ads} = \frac{\sqrt{m_2 m_3 m_1 R_2 R_{ct}\left(R_2 + R_{ct}\right)}}{m_2 m_3 m_1 R_2 R_{ct}^2} \tag{16}$$

$$m_1 = \left(-k_1 C_H - k_{-1} - k_2 C_H - k_{-2} - 4k_3\theta - 4k_{-3}(1-\theta)\right)(F/q)$$

$$m_2 = \left(-k_1 C_H - k_{-1} + k_2 C_H + k_{-2}\right)F$$

$$m_3 = \left((1/b_1)k_1 C_H(1-\theta) - (1/b_{-1})k_{-1}\theta - (1/b_2)k_2 C_H\theta + (1/b_{-2})k_{-2}(1-\theta)\right)(F/q)$$

Which are in agreement with data presented in tables 1 and 2.

The reaction rates of the Volmer, Heyrovsky and Tafel steps in the mechanism of the hydrogen evolution and the resulting total current value are all independently shown in figure 5, as calculated from the corresponding k_i values, calculated from impedance in a wide over potential region. From figure 5, one can conclude that the reaction mechanism is a consecutive combination of the Volmer and Heyrovsky step and that the Volmer step prevails over Heyrovsky step in low applied cathodic potential region. Reaction rate is controlled by the Heyrovsky reaction because of the much smaller k_2 value in this potential range as compared with the k_1 and k_3 values. In this overpotential domain the Tafel step is evidently potential dependent which is a direct consequence of the potential dependency of θ. At high negative potentials when the surface coverage of the electrode with H_{ads} reaches a constant value and the sequence of the three reaction rates are $v_1=v_2>v_3$, the mechanism of the hydrogen evolution is a consecutive combination of the Volmer and Heyrovsky steps with equal rates and the rate of the Tafel reaction being negligible. It should be noted that at high negative over potential range, the rate of Tafel step turns out to be independent of potential and the reaction rate is controlled by the Volmer step because of smaller k_1 value as compared with the k_2 values.

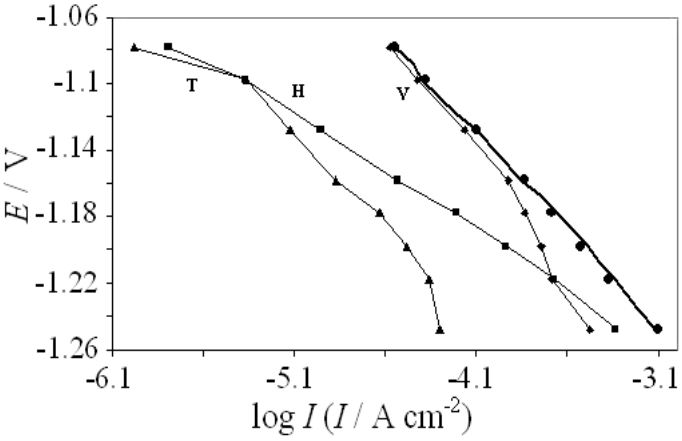

Figure-5
Potential dependence of the theoretically calculated individual rates for the Volmer (V), Heyrovsky (H) and Tafel (T) steps occurring simultaneously with the HER on Hg electrodes in 0.1 M H_2SO_4 solution at 25 °C. Theoretical polarization curve, obtained by summing individual curves is represented by full lines (•). Experimental data are presented by circled points (—)

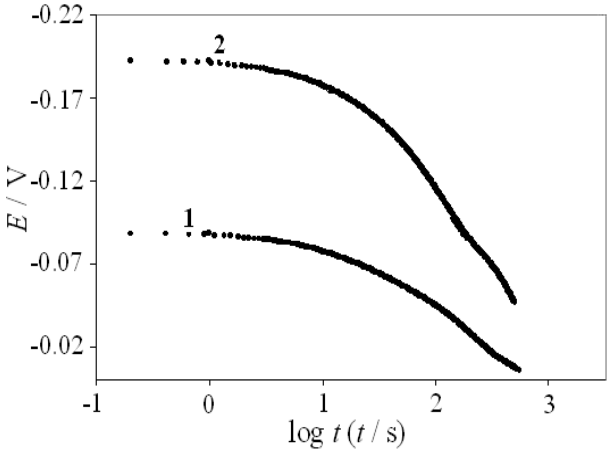

Figure-6
Potential against log time plot for the HER at Hg electrode reordered after interruption of 500 s applied current (1) 6×10^{-4}, (2) 1×10^{-3} mA cm^{-2} in 0.1 M H_2SO_4.

For more evidence, the process of absorption and comparing double-layer capacitance, open circuit potential transient

measurements were carried out[34]. For determination of the double-layer capacity the open circuit potential decay method was used. In this technique, potential decay is monitored after the interruption of the polarization current. The theory of this process was described by Conway and co-workers[18, 35,36] who proposed that in order to obtain the pseudocapacitances one has to calculate:

$$-(C_{dl} + C_{\Phi})\frac{d\eta}{dt} = I_o \exp\left(\frac{\alpha\eta F}{RT}\right) \quad (17)$$

where C_Φ is an operational pseudocapacitance, and I_o represents the exchange current density. In order to analyze this equation the derivative $d\eta/dt$ must be determined from the experimental potential decays curves. This derivative goes to zero at long time and the error of its determination increases with time. The potential-logarithm of time curve for Hg electrode which charged with different cathodic polarization currents for 500 s and recorded under open circuit regime are presented in figure 6. It is evident that the electrode does not relax to the equilibrium potential even after 350 s indicating the presence of a large pseudocapacitance.

At more negative over potential region where the pseudocapacitance is negligible, the double-layer capacitance can be determined. The corresponding *C-E* curves for Hg electrode obtained using Eq. (17) are presented in figure 7a and the double layer capacitance was found to be 4×10^{-5} F cm^{-2}. Corresponding *E*-log($d\eta/dt$) curves obtained after numerical differentiation is shown in figure 7b.

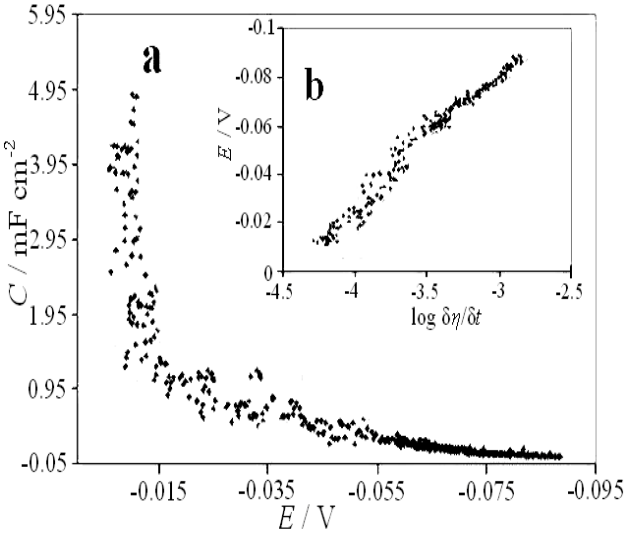

Figure-7 (a)
The capacitance against potential, (b) The potential against log($d\eta/dt$) plots for the HER at Hg electrodes in 0.1 M H_2SO_4

As can be seen in figure 7a, there is no clear maximum in *C*, but integration of *C* vs. *E* gives a charge that corresponds to more than one monolayer. Since it is difficult to cover an electrode with a film of H of more than one monolayer, the desorption of hydrogen during the potential decay results in very high *C* values around the open circuit potential but different to the values that follow from experimental impedance measurements. Upon interrupting the polarization current, the potential of the electrode will decrease with time because of the continuing passage of current across the double-layer causing discharge of the double-layer capacitance and also the pseudocapacitances due to the adsorbed and absorbed hydrogen.

Conclusion

In this study the kinetics of the hydrogen evolution reaction was investigated on Hg electrode in deaerated 0.1 M H_2SO_4 solution by the methods of impedance spectroscopy and open circuit potential as well as polarization measurements. The rate constants for individual reaction steps were determined. Moreover, by using these methods the potential dependence of hydrogen coverage and reaction rates of Volmer, Heyrovsky and Tafel steps during HER were evaluated. The results indicate that the main pathway of hydrogen evolution reaction at less negative potentials is the serial combination of Volmer and parallel Tafel and Heyrovsky steps. At highly negative potentials when the hydrogen coverage of the electrode surface reaches a relatively constant value the reaction proceeds through the Volmer-Heyrovsky mechanism with the rate determining step being the Volmer reaction. Open circuit potential for Hg at different charging currents shows that the duration of the slowly rising of potential increases with more cathodic charging current of hydrogen, which means that the higher the cathodic current the longer time is required to reach the equilibrium potential.

References

1. Kim H.K., Yang D.C., Jang I.S., Park C.N., Park C.J. and Choi J., Effects of pretreatment of LM-$Ni_{3.9}Co_{0.6}Mn_{0.3}Al_{0.2}$ alloy powders in a KOH/$NaBH_4$ solution on the electrode characteristics and inner pressure of nickel-metal-hydride secondary batteries, *Int. J. Hydrogen Energy,* **34**, 9570-9575 **(2009)**
2. Xu Y.H., He G.R. and Wang X.L., Hydrogen evolution reaction on the AB_5 metal hydride electrode, *Int. J. Hydrogen Energy* **28**, 961-965 **(2003)**
3. Jagadeesh B. Effects of Zinc and Tungsten Additions in Mn-Mo-O Eectrocatalyst for Hydrogen Production from Seawater Electrolysis, *Res. J. Chem. Sci.,* **1**, 13-119 **(2011)**
4. Liu B.H., Li Z.P. Zhu J.K. and Suda S., Influences of hydrogen evolution on the cell and stack performances of the direct borohydride fuel cell, *J. Power Sources* **183**, 151-156 **(2008)**
5. Lisnyak V.V., Ischenko E.V., Stratiichuk D.A., Zaderko A.N., Boldyrieva O.Yu., Safonova V.V. and Yatsymyrskyi A.V., Pt, Pd Supported on Niobium Phosphates as Catalysts

for the Hydrogen Oxidation, *Res. J. Chem. Sci.,* **3**, 30-33 **(2013)**

6. Huang Y., Wen Q., Jiang J. H., Shen G.L. and Yu R.Q., A novel electrochemical immuno sensor based on hydrogen evolution inhibition by enzymatic copper deposition on platinum nanoparticle-modified electrode, *Biosens. Bioelectron.* **24**, 600-605 **(2008)**

7. Islam M.M., Ferdousi B.N., Okajima T., Ohsaka T., A catalytic activity of a mercury electrode towards dioxygen reduction in room-temperature ionic liquids, *Electrochem. Commun.,* **7**, 789-795 **(2005)**

8. Ralph T.R., Hitchman M.L., Millington J.P. and Walsh F. C., The reduction of l-cystine in hydrochloric acid at mercury drop electrodes, *J. Electroanal. Chem.,* **587**, 31-41 **(2006)**

9. Rueda M., Compton R.G., Alden J. A. and Prieto F., Impedance voltammetry of electro-dimerization mechanisms: Application to the reduction of the methyl viologen di-cation at mercury electrodes and aqueous solutions, *J. Electroanal. Chem.,* **443**, 227-235 **(1998)**

10. Caetano J., Homem-de-Mello P., da Silva A.B.F. and Ferreira A.G., Avaca L A, Studies of the electrochemical reduction of atrazine on a mercury electrode in acid medium: An electrochemical and NMR approach, *J. Electroanal. Chem.* **608**, 47-51 **(2007)**

11. Montoya M.R., Pintado S. and Mellado J.M.R., Electrochemical reduction of imazamethabenz methyl on mercury and carbon electrodes, *Electrochim. Acta,* **55**, 3164-3170 **(2010)**

12. Saha M.S. and Ohsaka T., Electrode kinetics of the O_2/O_2^- redox couple at Hg electrode in the presence of PVC in aprotic media. *Electrochim, Acta,* **50**, 4746-4751 **(2005)**

13. Wisniewski A., Czerwinski W.K., Paklepa P., Wrona P.K. and Orlik M., The convection-driven non-additivity of the faradaic currents for the parallel reduction of some metal and hydrogen cations at the mercury electrode, *J. Electroanal. Chem.,* **623**, 120-128 **(2008)**

14. Gajek A. and Zakroczymski T. Long-lasting hydrogen evolution on and hydrogen entry into iron in an aqueous solution, *J. Electroanal. Chem.* **578**, 171-182 **(2005)**

15. Evard E., Gabis I. and Yartys V. A., Kinetics of hydrogen evolution from MgH_2: Experimental studies, mechanism and modeling, *Int. J. Hydrogen Energy,* **35**, 9060-9069 **(2010)**

16. Conway B.E. and Bai L., Determination of the adsorption behaviour of 'overpotential-deposited' hydrogen-atom species in the cathodic hydrogen-evolution reaction by analysis of potential-relaxation transients, *J. Chem. Soc. Faraday Trans.*1, **81**, 1841-1862 **(1985)**

17. Krstajic N.V., Grgur B.N., Mladenovic N.S., Vojnovic M.V. and Jaksic J.M., The determination of kinetics parameters of the hydrogen evolution on Ti---Ni alloys by *ac* impedance, *Electrochim. Acta,* **42**, 323-330 **(1997)**

18. Chen J.S., Diard J.P., Durand R. and Montella C. Hydrogen insertion reaction with restricted diffusion. Part 1. Potential step-EIS theory and review for the direct insertion mechanism, *J. Electroanal. Chem.*, **406**, 1-13 **(1996)**

19. Danaee I., Jafarian M., Forouzandeh F., Gobal F. and Mahjani M.G. Kinetic Interpretation of a Negative Time Constant Impedance of Glucose Electrooxidation, *J. Phys. Chem., B* **112**, 15933-15940 **(2008)**

20. Krishtalik L.I., Charge transfer reactions in electrochemical and chemical processes. New York, Plenum, **(1986)**

21. Danaee I., Jafarian M., Forouzandeh F., Gobal F. and Mahjani M.G., Electrochemical impedance studies of methanol oxidation on GC/Ni and GC/NiCu electrode, *Int. J. Hydrogen Energy,* **34**, 859-869 **(2009)**

22. Danaee I., Jafarian M., Mirzapoor A., Gobal F. and Mahjani M. G., Electrooxidation of methanol on NiMn alloy modified graphite electrode, *Electrochim, Acta,* **55,** 2093-2100 **(2010)**

23. Shan Z., Liu Y., Chen Z., Warrender G. and Tian J., Amorphous Ni-S-Mn alloy as hydrogen evolution reaction cathode in alkaline medium, *Int. J. Hydrogen Energy,* **33**, 28-33 **(2008)**

24. Chandran M. and Ramesh Bapu G.N.K., Electrodeposition of Nano Zinc - Nickel Alloy from Bromide Based Electrolyte, *Res. J. Chem. Sci.,* **3**, 57-62 **(2013)**

25. Danaee I. and Noori S., Kinetics of the hydrogen evolution reaction on NiMn graphite modified electrode. *Int. J. Hydrogen Energy,* **36**, 12102-12111 **(2011)**

26. Macdonald J.R., Note on the parameterization of the constant phase admittance element, *Solid State Ion.,* **13**, 147–149 **(1984)**

27. Danaee I., Kinetics and mechanism of palladium electrodeposition on graphite electrode by impedance and noise measurements, *J. Electroanal. Chem.,* **662**, 415-420 **(2011)**

28. Lasia A., Rami A., Kinetics of hydrogen evolution on nickel electrodes, *J. Electroanal. Chem.,* **294**, 123-141 **(1990)**

29. Krstajic N., Popovic M., Grgur B., Vojnovic M. and Sepa D., On the kinetics of the hydrogen evolution reaction on nickel in alkaline solution: Part I. The mechanism, *J. Electroanal. Chem.,* **512**, 16-26 **(2001)**

30. Shylesha B.S., Venkatesha T.V. and Praveen B.M. Corrosion Inhibition Studies of Mild Steel by New Inhibitor in Different Corrosive Medium, *Res. J. Chem. Sci.,* **1**, 46-50 **(2011)**

31. Prathibha B.S., Kotteeswaran P. and Bheema Raju V.Study on the Inhibition of Mild Steel Corrosion by Quaternary

Ammonium Compound in H2SO4 Medium, *Res. J. Rec. Sci.,* **2**, 1-10 **(2013)**

32. Manivannan M. and Rajendran S. Corrosion Inhibition of Carbon steel by Succinic acid – Zn2+ system, *Res. J. Chem. Sci.,* **1**, 42-48 **(2011)**

33. Bai L., Harrington D.A. and Conway B.E., Behavior of overpotential-deposited species in Faradaic reactions-II. *ac* Impedance measurements on H_2 evolution kinetics at activated and unactivated Pt cathodes, *Electrochim. Acta,* **32**, 1713-1731 **(1987)**

34. VracÏar L., Burojevic S. and Krstajic N., Unconventional temperature-dependence of Tafel slopes for the hydrogen evolution reaction at Pd-Ni electrode in alkaline solution, *J. Serb Chem. Soc.,* **63**, 201 **(1998)**

35. Harrington D. A. and Conway B. E., Kinetic theory of the open-circuit potential decay method for evaluation of behaviour of adsorbed intermediates: Analysis for the case of the H_2 evolution reaction, *J. Electroanal. Chem.,* **221**, 1-21 **(1987)**

36. Conway B.E., Bai L. and Tessier D.F., Data collection and processing of open-circuit potential-decay measurements using a digital oscilloscope: Derivation of the H-capacitance behaviour of H_2-evolving, Ni-based cathodes, *J. Electroanal. Chem.,* **161**, 39-49 **(1984)**